VOLATILE (S, C, F, Cl) CONTENTS OF ENSTATITE IN REDUCED METEORITES AS INDICATORS OF OXYGEN FUGACITY AND VOLATILE CONDITIONS IN THE EARLY SOLAR NEBULA. B. A. Anzures[1], S. W. Parman[1], J. S. Boesenberg[1], and R. E. Milliken[1]. [1]Department of Earth, Environmental, and Planetary Sciences, Brown University, Providence, RI, 02906. Email: brendan_anzures@brown.edu

Introduction: The early solar system experienced a wide range of oxygen fugacity (fO_2) conditions as recorded in different meteorites. Enstatite chondrites (EC) and aubrites are the most reduced meteorites indicated by their Fe-poor olivine and pyroxene, Si content of metal, and presence of minerals unique to reducing environments (e.g. (Mg,Ca)S). Based on Si in kamacite, EC's and aubrites record fO_2 between IW-3 to IW-8 [1,2]. Mercury [3], and perhaps the Earth [4], may also have formed at such low fO_2. However, enstatite and other components in EC's are not uniformally reduced and exhibit evidence of variable reduction of silicates [e.g. 5]. Therefore, it is important to determine fO_2 in reduced meteoritic silicates, which has previously been done on only one EL3 olivine using Cr X-ray absorption spectroscopy [6].

Experiments have shown that volatile solubility and speciation in silicate melts [7,8] and crystals [9] change dramatically at very reduced conditions. Thus, volatile measurements of meteoritic enstatite allow estimates of the fO_2 as well as the volatile gas and melt conditions during silicate equilibration. In this contribution we report on volatile (S, C, F, and Cl) content measurements of enstatite in reduced meteorites to explore these conditions and apply a S oxybarometer to these data to calculate fO_2 [9].

Samples: We studied 13 enstatite chondrite and achondrite meteorites including 3 EL's (EL3: MacAlpine Hills (MAC) 88136, Allan Hills (ALH) 85119; EL6: Hvittis), 4 EH's (EH3: Larkman Nunatak (LAR) 12252, LAR 12156, Sahara 97096; EH4: Indarch), 1 E-impact melt (EL-imp: Northwest Africa (NWA) 4301), and 5 aubrites (main group: LAR 04316, Cumberland Falls, Norton County; ungrouped aubrite: ALH 84011; anom. aubrite: Mount Egerton). Based upon published estimates, EH's (IW-7 to IW-8) are more reduced than EL's (IW-3 to IW-6), whereas aubrites record an intermediate fO_2 (IW-5 to IW-7) [1,2]. Samples were mounted in indium (except Hvittis was a thin section) and polished using 1.0 µm Al_2O_3.

Analyses: Volatile elements (S, C, F, Cl) were analyzed using the IMS 1280 SIMS instrument at Woods Hole Oceanographic Institute. A 30 μm^2 raster and 400 µm field aperture was used, designed to allow transmission of ions from only the innermost 5 µm diameter. Due to abundant metal±sulfide microinclusions, some volatile concentrations were corrected using the 0-intercept method of S and Cl (r^2 of 1 for MAC 88136 and LAR 12156; r^2 of 0.77 for LAR 12252). Enstatite and metal compositions were measured using the SX100 electron microprobe at Brown.

Results: Volatile abundances in enstatite are plotted against kamacite Si content as a proxy for reducing conditions (**Fig. 1**). The EL3 and EH3 samples exhibit high S irrespective of kamacite Si content. Aubrites are split between ALH 84011 and main group aubrites excluding Norton County (low Si kamacite and high S

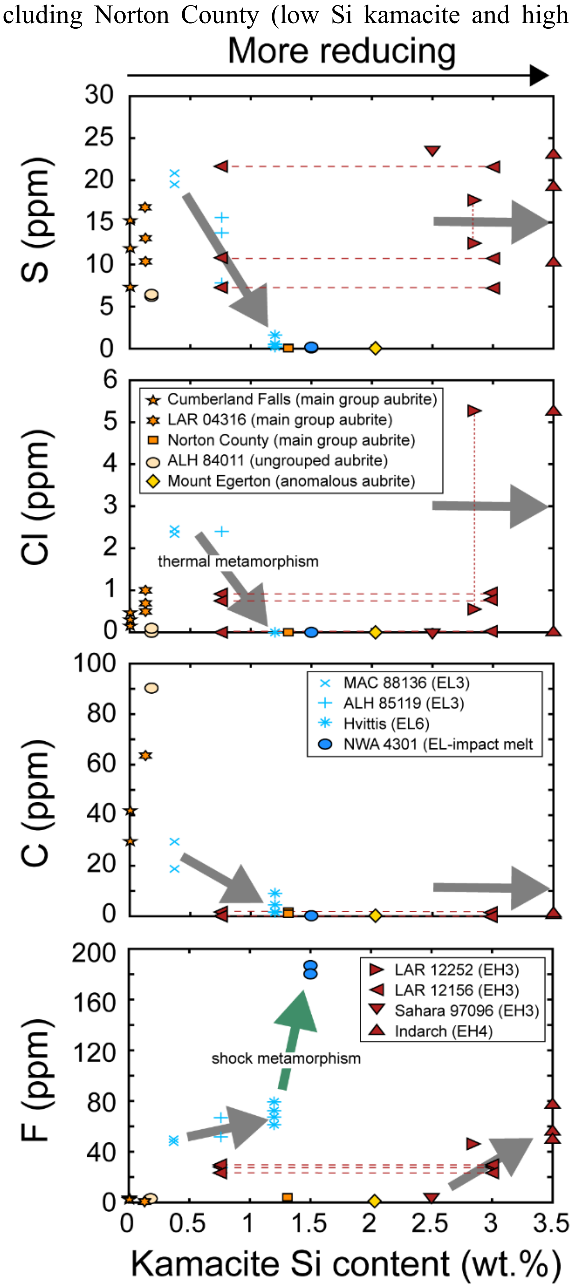

Figure 1. *Si in kamacite vs. S, Cl, C,, and F in enstatite. The horizontal dashed line represents two distinct Si kamacite compositions for LAR 12156 (0.77 wt.% and 3.00 wt.%). The vertical dashed line shows how the assumption of Cl content affects LAR 12252's S content.*

enstatite) versus Norton County and anomalous aubrite Mount Egerton (high Si kamacite and low S enstatite), roughly consistent with two previously identified REE groups [10]. C is quite low in most meteorites except for EL's and a few aubrites even though they contain graphite; C could have reached saturation after silicate crystallization from metal exsolution during lower temperature metamorphism [11]. F is very abundant with concentrations up to ~180 ppm. The high scatter of F suggests it was undersaturated and mobile. With increasing metamorphism feldspar grains (the main host of F in reduced meteorites) coarsen from <2µm to up to 200 µm [12], which may diffuse F into enstatite. In fact, EL-impact melt NWA 4301 has rare feldspar microinclusions within enstatite [13]. Cl is scarce with abundances below 6 and most below the 0.001 ppm SIMS detection limit for all meteorites implying low Cl stability in enstatite formed under very reducing conditions.

Table 1. Major element composition of enstatite

	FeO	CaO	Al_2O_3
MAC 88136	0.22-8.25	0.18-0.42	0.17-0.36
ALH 85119	0.14-2.46	0.16-0.32	0.15-0.24
Hvittis	0-7.98	0.80-0.90	0.19-0.25
NWA 4301	0.24-0.72	0.25-0.40	0.05-0.20
LAR 12252	0.69-2.13	0.11-0.38	0.09-0.48
LAR 12156	0.83-9.93	0.07-4.19	0.04-4.42
Sahara 97096	0.65-1.88	0.14-0.41	0.19-0.50
Indarch	0.86-1.60	0.14-0.20	0.21-0.28
Cumberland Falls	0.03-0.12	0.31-0.36	0.07-0.08
Norton County	0-0.05	0.30-0.60	0.01-0.05
LAR 04316	0.01-0.07	0.10-0.13	0.01-0.05
ALH 84011	0.00-0.07	0.18-0.44	0.02-0.55
Mount Egerton	0.01-0.02	0.37-0.55	0.04-0.08

EL's: EL's contain 30-200 µm size enstatite that have abundant metal microinclusions. Estimates of fO_2 range from IW-2.69 to -7.08 (**Fig. 2**), which is a larger range than fO_2 from kamacite (IW-3 to IW-6) [1]. The largest fO_2 range within a single meteorite is observed in ALH 85119 (IW-4.84 to IW-6.40). Excitingly, the fO_2 of MAC 88136 (IW-6.93 and IW-7.08) is consistent with the upper limit of IW-6 in one forsterite grain [6]. With increasing metamorphism S, Cl, and C are lost implying these elements are loosely bonded in meteoritic enstatite (EL3 → EL6 **Fig. 1**).

EH's: EH's contain 30-200 µm size enstatite that have abundant metal/sulfide microinclusions. Similar to EL's, estimates of fO_2 range from IW-4.71 to -7.27, (**Fig. 2**), which is a larger range than fO_2 from kamacite (IW-7 to IW-8) [1]. Considerable fO_2 variation is observed in LAR 12156 (IW-4.71 to IW-7.16).

Aubrites: Aubrites contain mm-cm size fractured enstatite. Estimates of fO_2 range from IW-2.64 to -6.64 (**Fig. 2**), which is a larger range than fO_2 from kamacite (IW-5 to IW-7) [2]. There is little fO_2 variation within meteorites (σ<0.67). Aubrites also contain higher S enstatite associated with lower Si in kamacite (less reducing conditions). This is opposite the expected trend, but the Si content may be reflective of metamorphism and/or S may have been lost through fractionation of metal/sulfide and enstatite in the aubrite parent body.

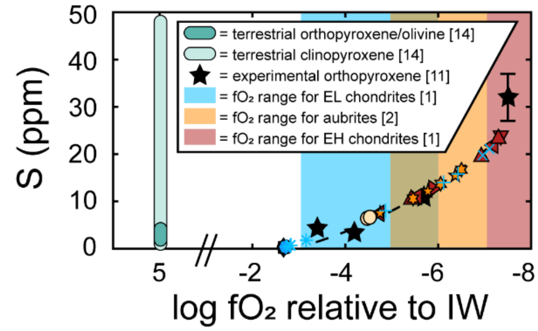

Figure 2. *fO_2 relative to IW vs. S in enstatite. Experiments where the fO_2 conditions are known define the black dashed curve for volatile saturation in orthopyroxene. Meteoritic S agrees with estimated fO_2 from kamacite, although all meteorite groups skew towards more oxidizing conditions.*

Implications for early solar nebular conditions: EL's, EH's, and aubrites likely formed in a similar location in the solar nebula indicated by similarities in oxygen isotopes [10] and reduced nature. Reduction has been attributed to 1) condensation in a high C/O gas [e.g. 15], 2) sulfidization of more oxidized material in a H-poor, C- and S-rich gas at IW-6 to 8 in the case of EC's [e.g. 16], and 3) reduction of more oxidized material during thermal metamorphism [e.g. 17].

Enstatite volatile abundances offer insights into the solar nebula during meteorite formation. The strong correlation between S and Cl in both the enstatite and many metal/sulfide microinclusions in EC's indicate high Cl fugacity and reactivity during the sulfidization event. This is in agreement with high bulk Cl in EC's compared with other meteorite groups [18].

Finally, the S oxybarometer was useful in calculating the fO_2 of individual enstatite grains in a suite of reduced meteorites. Enstatite fO_2's for each meteorite group were similar to but skewed toward more oxidizing conditions than fO_2 from kamacite and also varied up to 2.5 log units in a given meteorite. Both of these observations are consistent with variable reduction of a more oxidizing precursor material.

References: [1] Fogel R. A. et al. (1989) *GCA 53*, 2735-2746. [2] Casanova I. et al. (1993) *GCA 57*, 675-682. [3] McCubbin F. M. et al. (2012) *GRL, 39*, 1-5. [4] Javoy M. et al. (2010) *EPSL, 293*, 259-268. [5] Lusby D. et al. (1987) *JGR, 92*, E679-E695. [6] McKeown D. A. et al. (2014) *Amer. Min., 99*, 190-197. [7] Zolotov M. Y. (2011) *Icarus, 212*, 24-41. [8] Anzures B. A. et al. (2018) *LPSC XLIX*, Abstr #1694. [9] Anzures B. A. et al. (2019) *LPSC L*, Abstr #2179. [10] Barrat J. A. et al. (2016) *GCA, 192*, 29-48. [11] El Goresy A. et al. (2017) *MaPS, 52*, 781-806. [12] Brearley A. J. & Jones R. H. (1998) *RIMG, 36*, 1-398. [13] Boesenberg J. S. (2014) *LPSC XLV*, Abstr #1486. [14] Callegaro S. et al. (2014) *Geology 42*, 895-898. [15] Larimer J. W. (1975) *GCA, 39*, 389-392. [16] Lehner S. W. (2013) *GCA, 101*, 34-56. [17] Zhang Y. et al. (1995) *GCA, 100*, 9417-9438. [18] Rubin A. E. & Choi B.-G. (2009), *Earth, Moon, & Plan., 105*, 41-53.